LOW-POWER SIMPLEX ULTRASOUND COMMUNICATION FOR INDOOR LOCALIZATION

Alexander Ens, Leonhard M. Reindl

University of Freiburg, Germany
alexander.ens, reindl@imtek.uni-freiburg.de

Thomas Janson, Christian Schindelhauer

University of Freiburg, Germany
janson, schindel@informatik.uni-freiburg.de

ABSTRACT

We propose an ultrasound communication system designed for time difference of arrival (TDOA) based indoor localization. The concept involves an infrastructure of stationary and independent senders tracking mobile receivers. The main goal is pure line-of-sight (LOS) communication for correct localization. When ignoring the reception energy of multipaths the transmission range is reduced to 20 meters and we need more devices to cover the same area (0.03 devices/m^2). Thus, for cost-effectiveness and easy installation, we focus in the sender design on low power consumption for long battery or even energy independent operation. Moreover, we use the energy efficient $\pi/4$-DQPSK modulation technique to send 8 data bits in 3.5 ms. An identifier in each message along with the reception time can be used for TDOA localization. The frame synchronization error for a distance of 20 m at 3 dB SNR is 11.2 ns. Thus, for speed of sound the distance measurement error is 3.7 μm.

***Index Terms*—Ultrasound, DQPSK, Transmission, ToA, TDOA, Localization, Communication, Line of Sight, Class-E Amplifier**

I. INTRODUCTION

Indoor localization of things enables a wide field of new possibilities like navigation and location-specific information in the consumer market or industrial field (e.g. process control in warehouses). Global navigation satellite systems (GNSS) (e.g. Galileo, GPS or GLONASS) do not work indoors. Instead, local solutions have to be installed inside the buildings. This work presents wireless signal transmission with ultrasound for time of arrival (TOA) measurements and data transfer, both needed in indoor localization systems, e.g. our algorithm [1] for tracking mobile receivers with unsynchronized stationary senders.

Reliable localization profits from precise and unambiguous distance measurements in terms of a unique mapping of a measurement value to a distance between devices. Whereas radio reaches through walls and floors making for example the localization of the correct floor more ambitious, ultrasound has high attenuation in matter and a high reflection property, for instance near full reflection for concrete. So when using ultrasound, localization is simplified to local areas like rooms or corridors in warehouses. Received signal strength indicator (RSSI) values in radio communication are subject to high fluctuations, due to environment-dependent multipath propagation [2]. Thus, reference points in the area for localization have to be taken to clear up inconclusive measurements. This can be time-consuming and costly and has to be updated when the environment changes, for instance with new obstacles. In contrast, the line-of-sight (LOS) path is the shortest path between sender and receiver and the transmission delay is linear to the path length from sender to receiver.

In our work, we use low-frequency (40.8 kHz) ultrasound for simplex data transmission. Furthermore, the synchronization of the transmission frame is used for exact measurement of TOA. The transmitted data includes an identifier of the sender and the temperature at its location. The temperature is used to increase the precision of the propagation time from sender to receiver where the speed of sound is subject to temperature influences. The senders are installed on the ceiling and the trackable receivers are mobile.

In addition, the low power design of our stationary senders enables feasible indoor photovoltaic power supply [3]. Thus, the mounting of the senders is flexible and cost-effective without the requirement of external power supply. Low power is achieved by combining a high efficiency class-E amplifier and $\pi/4$-DQPSK modulation with high data rates and thus short transmission times. However, the pulse shape to produce the carrier is a rectangle instead of a raised-cosine and needs a higher frequency bandwidth. To cope with intermodulation distortion (IMD) we use a guard interval between symbols. Including our localization algorithms of [1] we do not need an additional control channel via RF or wire and hence the system is applicable in industrial environments where RF communication is not possible.

II. RELATED WORK

Ultrasound seems an obvious technology for localization since ultrasound and distance measurement have quite a history, e.g. ultrasound parking assist with airborne ultrasound also with 40 kHz. In [4], [5] the ultrasound senders modulate the data by binary shift keying (BSK). However, to overcome the multipath propagation, they use ultrasound pulse lengths

of up to 100 ms [6], [7] and code division multiplex access (CDMA) codes (e.g. Kasami code and Barker code).

When the schedule for sending of the senders/beacons is unknown or not centrally controlled, sender identification and interference avoidance can be achieved by assigning an exclusive channel (carrier frequency). However, each receiver requires a broadband transceiver and with low exploitation of each channel the number of available channels in the limited frequency spectrum might be a problem [8]. Holms et al. present in [9] for an indoor positioning system ultrasound communication with frequency shift keying (FSK) modulating the sender identifier (ID). Chirp spread spectrum (CSS) modulation with broadband ultrasound transceivers is also used for localization (e.g. [10]) to improve the precision of TOA measurements for multipath channels. For ultrasound narrowband transceivers, we developed a CSS and FSK combined modulation scheme [11]. Nevertheless, the system also uses multipath propagation.

On the contrary, senders can also modulate their sender ID on a single carrier frequency. The authors of [12] show ultra-wideband ultrasound communication for distances of up to 2 m. The data is modulated using QPSK and the system achieves a transmission rate of up to 1.3 Mbit/s. They show a laboratory system, where the signal is processed on a computer. In contrast, in our system the mobile device can demodulate the signal and estimates the data on an ARM Cortex M4 micro-controller.

III. SYSTEM DESCRIPTION

The simplex ultrasound transmission system is designed to determine the TDOA in our indoor localization system [1]. Figure 1 shows the principle of the TDOA localization system. In our setting we have an infrastructure with stationary and independent ultrasound senders and a (set of) mobile device(s) which can track themselves when moving. For that,

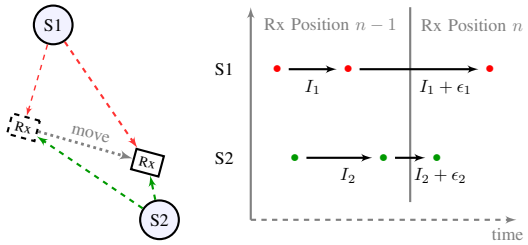

Fig. 1. Principle of the TDOA localization system [1].

each sender repeats the packet containing its ID in a fixed interval and when the mobile device changes the distance to a sender, the interval (I_1, I_2) slightly changes with Doppler-shift. With a stable clock at the receiver and several packets of the same sender received at different positions, we can determine time difference of arrival (TDOA) ϵ for those places. Thus, the senders can operate independent and unsynchronized and repeat their packets with an interval proportional to the update rate for localization. We do not apply collision detection or avoidance. We assume that enough transmissions are successful when different senders have different transmission intervals, whereby a sender can derive the interval from the sender ID. Since the mobile devices are only in reception mode, the tracking system can cope with an unlimited number of mobile devices tracking themselves.

In the further analysis we assume an attenuation of the amplitude with $1/d$ for distance d and the velocity of sound is $v_s = 330\,\frac{\mathrm{m}}{\mathrm{s}}$. Walls are very good reflectors for ultrasound [13] with a reflection coefficient $\rho_{\mathrm{Wall}} \approx 1$.

Imagine an indoor scenario with large halls (e.g. in shops or warehouses) where a receiver is mobile on the floor with distance $d_{\mathrm{Rx,W}}$ to the next wall. A sender is placed on the ceiling with mounting height h_{Mon} and distance $d_{Tx,w}$ to the same wall (see Figure 2). The pure LOS echo free signal duration is then

$$\begin{aligned}\tau_{ef} &= v_s\left(d_{Rx,w}+d_{Tx,w}\right)\sqrt{1+\frac{h_{\mathrm{Mon}}}{d_{Rx,w}+d_{Tx,w}}} \\ &\quad -v_s\sqrt{h_{\mathrm{Mon}}^2+\left(d_{Tx,w}-d_{Rx,w}\right)^2}\,. \end{aligned} \tag{1}$$

For $d_{Tx,w} = 6\,\mathrm{m}$, $h_{\mathrm{LoS}} = 6\,\mathrm{m}$ and $d_{Rx,w} = 1\,\mathrm{m}$ the echo free signal duration is $\tau_{\mathrm{ef}} = 6\,\mathrm{ms}$. Therefore, the LOS signal arrives first at the receiver, followed by the reverberation of up to 40 ms. Subsequently, after the LOS signal, the receiver discards the followed signal for 40 ms and the multipath signal is not used.

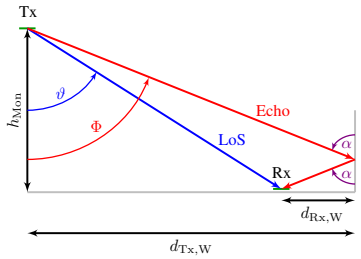

Fig. 2. Visualization of LoS and the shortest echo signal.

For ultrasound transmission, we use piezo-electric transducers with a resonance frequency of $f_r = 40.8\,\mathrm{kHz}$ and a maximum sound pressure level (SPL) of 120 dB (reference sound pressure $20\,\mu$P) at a distance of 0.3 m. The sound absorption by air increases with the used frequency [14], [13]. Therefore, data transmission with low frequencies attains a better SNR (Signal to Noise Ratio) for long distances up to 20 meters and we choose the lower end of the ultrasound frequency band for our transmission scheme. To avoid intermodulation distortion when using narrow bandwidth transducers and pulse modulated signals, a guard interval is added between the symbols.

III-A. Sender

For simplex communication, we optimize the hardware of the sender for energy efficiency and a cost-effective design. The sender is powered with 10 V and consumes 24 mA in the transmission period and 150 μA in the sleep period. The mean power consumption for a frame sending frequency $\frac{1}{I_P} = f_P \leq 10$ Hz and a transfer time of $\tau_{Tx} = 3.5\,\mathrm{ms}$ per frame is therefore

$$P(f_P) = (1 - \tau_{Tx} f_P)\, 1.5\,\mathrm{mW} + \tau_{Tx} f_P 240\,\mathrm{mW}\,. \quad (2)$$

At a moderate interval of 1 Hz the power consumption is 2.3 mW which can be provided by an indoor photovoltaic generator.

Figure 3 shows the diagram of the sender. A low power micro-controller generates the transmission signal by generating rectangle pulses. The time values between the pulses for the $\pi/4$-DQPSK modulation are stored in a look-up table. An amplifier generates a differential signal with a voltage swing of $U_{pp} = 20\,\mathrm{V}$ (with the values $\{-10\,\mathrm{V}, 10\,\mathrm{V}\}$) and drives the piezo-electric transducer (Murata MA40S4S) in its resonance frequency f_r. Consequently no digital to analog converter (DAC) and ineffective class-AB amplifier is needed. The efficiency of the pulse modulated class-E amplifier is about 90 % compared to the 40 % of the class-AB amplifier [15]. Furthermore the amount of devices, the complexity and hardware costs are reduced. Moreover, the sender costs are below 10 Euro.

Figure 4 shows the schematic of the signal generation. The amount of pulse values for the timer is

$$N = \gamma_{\mathrm{odd}}\,(2 \cdot \tau_{\mathrm{SG}} \cdot f_r) \quad (3)$$

whereat function γ_{odd} rounds to the next odd number and τ_{SG} is the time duration of the symbol plus guard interval. The pulse length value for the timer is calculated with the micro-controller timer frequency f_{T} to $\delta = \lfloor f_T / (2 \cdot f_r) \rfloor$. The value δ is added to the compare register value c_r for every output toggling. After n toggling points, the phase shift is added to the register c_r. Further, the pulse lengths for the phase shifts between the symbols are calculated as

$$\vartheta(n) = \left\lfloor \frac{f_{\mathrm{T}} \cdot (2n+5)}{8 \cdot f_r} \right\rfloor, \qquad \forall n \in \{0, \ldots, 3\}\,. \quad (4)$$

Indeed, the phase shift includes a half term of the sine to ensure the register loading of the micro-controller in time. The $\pi/4$ phase shift is included in the phase calculation in Equation (4).

III-B. Receiver

Figure 5 shows the diagram of the receiver and the signal processing. The piezo-electric transceiver (Murata MA40S4R) transforms the acoustic signal into electrical values. The weak received signal is amplified by a low noise amplifier (LNA) and digitalized by an analog-to-digital converter (ADC). An additional power meter provides

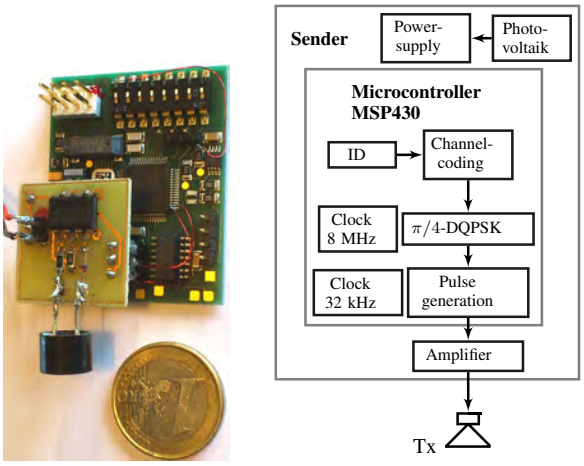

Fig. 3. Photo and schematic diagram of the sender.

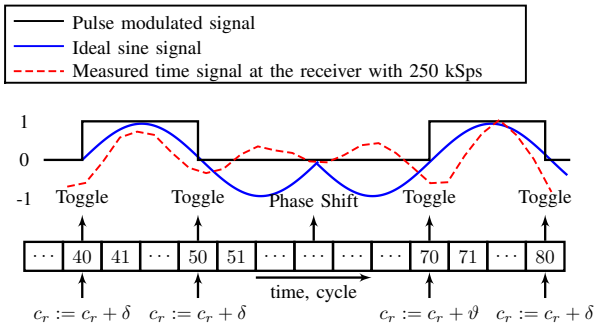

Fig. 4. Diagram for sine generation using pulse modulation. The signal is distorted between two symbols (IMD).

the current signal strength of the ultrasound transceiver to the comparator. Further, the comparator detects the beginning of a frame by comparing the signal strength with a threshold. Hence, the micro-controller sleeps until the comparator triggers the signal processing and we avoid energy-intensive signal processing when no signal is present. The microcontroller STM32F407 with ARM Cortex M4F samples the analog signal to digital values with sampling frequency $f_{\mathrm{sample}} = 500\,\mathrm{kHz}$. Furthermore, the complete signal processing for demodulation is calculated with floating point accuracy on the microcontroller. The signal is correlated (symbol $\star$) with the complex reference signal to estimate the phase. After synchronization, the symbols are estimated from the phase. The decoded data and the SNR is transmitted by the UART (universal asynchronous receiver transmitter) interface to an embedded computer for further processing. The input of the localization software then is the reception time and the sender ID plus temperature to determine the TDOA values and subsequently the position. The (time critical) real time signal processing for synchronization to the received signal and data demodulation

is done on the ARM CORTEX M4F. On the contrary, the computationally complex localization software is executed on a separate ARM Cortex A9 with an embedded real-time Linux operating system.

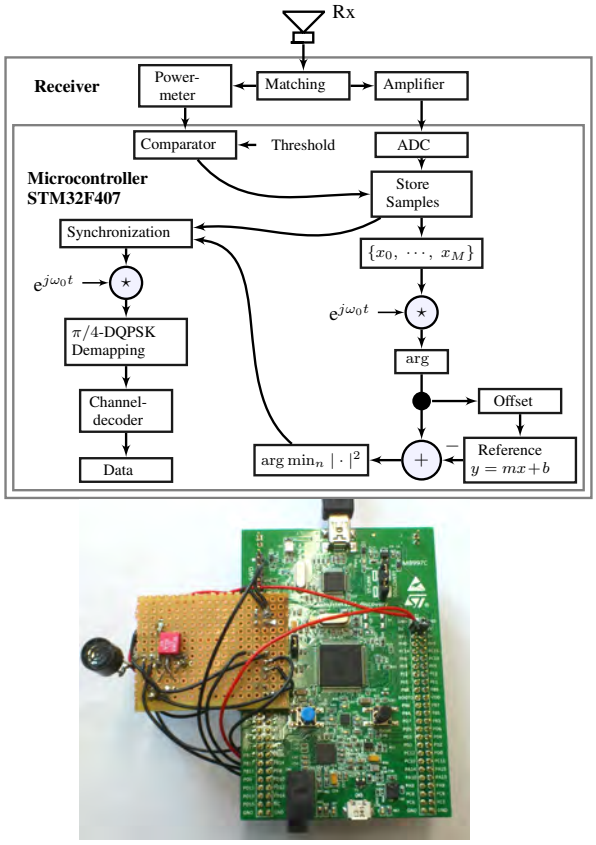

Fig. 5. Schematic diagram and photo of the receiver.

IV. SYNCHRONIZATION

Precise localization depends on the accuracy of the frame synchronization. Therefore, the synchronization is based on the estimated signal phase $\hat{\phi}$. However, the power meter in the system triggers the ADC sampling to start with a first imprecise synchronization which reduces the computation time[1]. The precise synchronization point is then calculated from the phase variance

$$\mathrm{Var}\left(\hat{\phi}_M(k)\right) = \frac{1}{M}\sum_{x=k}^{M+k}\left(\hat{\phi}(x) - \hat{\bar{\phi}}_M(k)\right)^2 \tag{5}$$

with the windowed mean

$$\hat{\bar{\phi}}_M(k) = \frac{1}{M}\sum_{x=k}^{M+k}\hat{\phi}(x)\ . \tag{6}$$

[1]In result, this saves energy or provides more computing performance to the localization software on the non-dedicated hardware.

In addition, the minimum of the variance gives us the synchronization point

$$n_{\mathrm{sync}} = \arg\min_k \mathrm{Var}\left(\hat{\phi}_M(k)\right)\ . \tag{7}$$

IV-A. Cramér-Rao Lower Bound

We assume a linear channel with only the LOS signal and additive white Gaussian noise with normal distribution $\mathcal{N}\left(0, \sigma^2\right)$ and standard deviation σ. The Cramér-Rao lower bound for synchronization can be derived from Equation 7 to

$$\mathrm{Var}\left(\Phi_{\tau_{\mathrm{sync}}}\right) \geq \frac{1}{M \cdot N \cdot \mathrm{SNR} \cdot \omega_r^2} \tag{8}$$

whereat the symbol duration is $\tau_s = 0.5\,\mathrm{ms}$, the amount of samples per symbol is $N = f_{\mathrm{sample}} \cdot \tau_s$, N the amount of samples for phase estimation and $M := N$. Therefore, Equation (8) can be rewritten as

$$\mathrm{Var}\left(\Phi_{\tau_{\mathrm{sync}}}\right) \geq \frac{1}{f_{\mathrm{sample}}^2 \cdot \tau_s^2 \cdot \mathrm{SNR} \cdot \omega_r^2}\ . \tag{9}$$

For the given numerical values we have a minimum standard deviation $\mathrm{SD}\left(\Phi_{\tau_{\mathrm{sync}}}\right) \geq \frac{15.9 \cdot 10^{-9}}{\sqrt{\mathrm{SNR}}}\,\mathrm{s}$. With the speed of sound v_s we get a standard deviation of the distance of $\mathrm{SD}\left(d_{\tau_{\mathrm{sync}}}\right) \geq \frac{5.25 \cdot 10^{-6}}{\sqrt{\mathrm{SNR}}}\,\mathrm{m}$.

V. MEASUREMENT

We performed measurements with the hardware presented in Chapter 3 and sufficiently large distances to walls (see Fig. 2). Figure 6 top shows the variance of the phase over time, calculated with Equation (5). The minimum of the variance at time 0.45 ms is the synchronization point of the frame. The simulated signal is plotted with a dashed red curve. The black curve shows the measurement result for the distance 0.3 m. The blue curve with circles shows the measured results for 9 m transmission distance. Figure 6 middle shows the phase over time. The phase shifts are as expected $\pi/4$, $-\pi 3/4$, $-\pi/4$, and $-\pi 3/4$. The phase shifts in the guard intervals between the symbols are marked light yellow and the stable phases for symbol estimation are marked light green. Figure 6 bottom shows the SNR over time which is higher than 10 dB for 9 m distance during the symbol frames. Further, the mean of the SNR is 15 dB. For a distance of 20 m the SNR would decrease by 7 dB according to the signal decay with $(20 \cdot \log_{10}\left(\frac{20}{9}\right))$. Therefore, the mean SNR is 8 dB (minimum SNR 3 dB), which is feasible for our transmission system.

VI. CONCLUSION

We present an ultrasound transmission system for TDOA localization, which is optimized for an infrastructure with low power and cost-effective stationary senders. Therefore, our pulse modulation system achieves the same performance as analog sine generation. It combines three key features: for energy efficiency the signal is generated by a micro-controller with a pulse modulation, we use narrow band

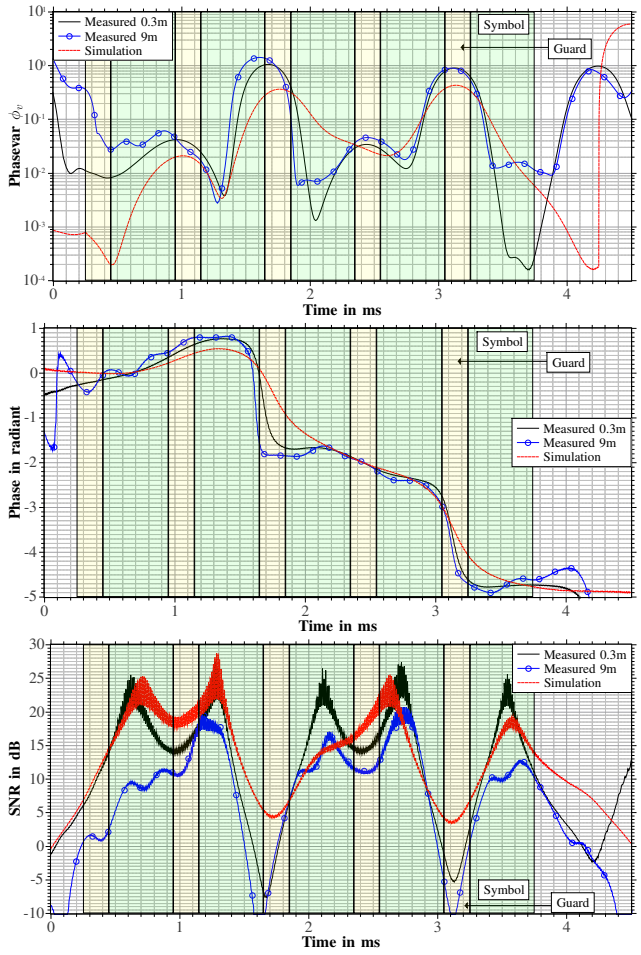

Fig. 6. Results of measured transmission over 0.3 m and 9 m. Top: Phase variance over time. Middle: Phase over Time. Bottom: SNR over Time.

piezo-electric transceivers to band pass the pulse modulated signal, and the signal is modulated by $\pi/4$-DQPSK to achieve high data rate for pure LOS communication and correct localization. With the shown precision of the frame synchronization the distance error corresponding to the transmission delay is smaller than 3.7 μm. Moreover, the low power design enables feasible indoor photovoltaic power supply and reduced installation costs.

REFERENCES

[1] J. Bordoy, P. Hornecker, J. Wendeberg, R. Zhang, C. Schindelhauer, and L. Reindl, "Robust tracking of a mobile receiver using unsynchronized time differences of arrival," in *Int. Conf. on Indoor Positioning and Indoor Navigation*, 2013.

[2] C. Medina, J.C. Segura, and S. Holm, "Feasibility of ultrasound positioning based on signal strength," in *Int. Conf. on Indoor Positioning and Indoor Navigation*, 2012.

[3] M. Freunek, M. Freunek, and L.M. Reindl, "Maximum efficiencies of indoor photovoltaic devices," *IEEE Journal of Photovoltaics*, vol. 3, pp. 59–64, Jan. 2013.

[4] H. Yoshiga, A. Suzuki, and T. Iyota, "An information addition technique for indoor self-localization systems using SS ultrasonic waves," in *Int. Conf. on Indoor Positioning and Indoor Navigation*, 2012.

[5] D. Ruiz, E. Garcia, J. Urena, D. de Diego, D. Gualda, and J.C. Garcia, "Extensive ultrasonic local positioning system for navigating with mobile robots," in *10th Workshop on Positioning Navigation and Communication*, 2013.

[6] C. Medina, J.C. Segura, and A. De la Torre, "A synchronous TDMA ultrasonic TOF measurement system for low-power wireless sensor networks," *IEEE Transactions on Instrumentation and Measurement*, vol. 62, no. 3, pp. 599–611, Mar. 2013.

[7] Seong Jin Kim and Byung Kook Kim, "Dynamic ultrasonic hybrid localization system for indoor mobile robots," *IEEE Transactions on Industrial Electronics*, vol. 60, no. 10, pp. 4562–4573, Oct. 2013.

[8] William C Jakes, *Microwave mobile communications*, IEEE Press, Piscataway, NJ, 1993.

[9] S. Holm, O.B. Hovind, S. Rostad, and R. Holm, "Indoors data communications using airborne ultrasound," in *IEEE Intern. Conf. on Acoustics, Speech, and Signal Processing*, 2005, vol. 3, pp. 957–960.

[10] Y. Itagaki, A. Suzuki, and T. Iyota, "Indoor positioning for moving objects using a hardware device with spread spectrum ultrasonic waves," in *Int. Conf. on Indoor Positioning and Indoor Navigation*, 2012.

[11] Alexander Ens, F. Höflinger, J. Wendeberg, L. M. Reindl, and C. Schindelhauer, "Indoor positioning using ultrasonic waves with CSS and FSK modulation for narrow band channel," in *Int. Conf. on Indoor Positioning and Indoor Navigation*, 2013.

[12] Chuan Li, D.A. Hutchins, and R.J. Green, "Short-range ultrasonic communications in air using quadrature modulation," *IEEE Transactions on Ultrasonics, Ferroelectrics and Frequency Control*, vol. 56, no. 10, pp. 2060–2072, Oct. 2009.

[13] "ISO 9613-1:1993, acoustics – attenuation of sound during propagation outdoors – part1," .

[14] Hans-Rolf Tränkler, *Taschenbuch der Messtechnik mit Schwerpunkt Sensortechnik*, Oldenbourg, 1996.

[15] David P. Kimber, *Class E amplifiers and their modulation behaviour*, Ph.D., University of Birmingham, July 2006.